AKADÉMIAI KIADÓ

Pollack Periodica • An International Journal for Engineering and Information Sciences

19 (2024) 1, 13–18

DOI: 10.1556/606.2023.00946


ORIGINAL RESEARCH PAPER

# Experimental study of failure of glulam-concrete composite beams

Tamás Juhász[1*], Yishi Lee[2], Rose Holtzman[2] and Jeno Balogh[2]

[1] Structural Diagnostics and Analyses Research Team, Department of Civil Engineering, Institute of Smart Technology and Engineering, Faculty of Engineering and Information Technology, University of Pécs, Pécs, Hungary

[2] Department of Engineering, College of Aerospace, Computing, Engineering, and Design, Metropolitan State University of Denver, Denver, CO, USA

Received: September 18, 2023 • Revised manuscript received: November 25, 2023 • Accepted: November 30, 2023
Published online: February 7, 2024

**ABSTRACT**

This paper is dedicated to the memory of Dr. Miklós Iványi, who instilled in the authors an appreciation for experimental investigations, which are foundational to understanding material and structural behavior. Timber-concrete composite structures are increasingly adopted for new buildings due to their favorable sustainability parameters and the increased availability of cross laminated timber. For larger spans, however, solid timber floors lead to higher timber volumes and the use of glulam beams may become necessary for a more efficient use of wood. This paper presents laboratory tests of glulam-concrete composite beams and is the first in a series of two papers on investigating the associated failure mechanisms. Three full-scale glulam-concrete beam specimens were studied. The glulam and concrete are monolithically interconnected using a continuous layer of adhesive. Shear reinforcement was added to the glulam beams to allow for failure mode control. Static load tests to failure were conducted along with acoustic emission monitoring to track the progression of the failure. The results indicate that the shear reinforcement of the glulam layer affects the load capacity of the composite beam through shifting the failure from a shear to a tension failure mode. Similar glulam-concrete beams can enable larger span applications for buildings and bridges while maintaining an attractive sustainability performance.

**KEYWORDS**

glulam-concrete members, experimental investigations, acoustic emissions

## 1. INTRODUCTION

Over the past decades several methods for interconnecting a timber and a top concrete layer in beams were developed achieving various levels of efficiency of composite action [1]. The highest composite stiffness was observed in the solutions, which used adhesives to connect the two layers. This is attributed to the high rigidity of the adhesive layer along with having a connection continuous on the full length of the beam [2–5]. In composite floors using Cross Laminated Timber (CLT), adhesives can be used to connect a concrete layer on the top with no need for mechanical connectors or notches, unless a ductile behavior is desired [6, 7]. In this paper, Glulam-Concrete (G-C) beams are studied that are intended for larger span applications in which a CLT based solution would lead to an excessively massive floor. Reinforcing steel bars glued into the glulam are used for strengthening the glulam beams in shear. Papers [8, 9] report immense experience existing in using glued-in bars in the repair and strengthening of timber beams both softwood and hardwood, as well as in connecting concrete slabs to floor beams.

## 2. EXPERIMENTAL PROGRAM

Laboratory investigations of G-C laminated structural beam members for floors or bridges were conducted in the Structural Laboratory at Metropolitan State University of Denver.

*Corresponding author.
E-mail: juhasz.tamas@mik.pte.hu

The experimental program consisted of static load tests to failure with an array of accelerometers for Acoustic Emission (AE) monitoring to track the emissions due to failure within the specimen [10–12].

## 2.1. Specimen design and load test setup

Three G-C beam specimens with a length of 4.877 m (192 in) were built and setup with a span of 4.623 m (182 in). The timber layer consists of an APA-The Engineered Wood Association-rated 24F-V4 glulam beam, with Douglas fir material and unbalanced layering. The nominal glulam beam width and height is 79.4 mm (3.125 in) and 381 mm (15 in), respectively. The 76.2 mm (3 in) concrete layer consists of a C40/50 (40 N $mm^{-2}$, 6000 psi) basalt fiber reinforced normal weight concrete. The timber and the concrete layer are interconnected with a Dayton Superior Sure Bond J58 two component, high modulus, moisture-tolerant adhesive [9]. The adhesive was applied on the top of the glulam in two layers, 10–15 min apart then the fresh concrete was placed in the form 10–15 min later. The glulam is embedded into the concrete by 12.7 mm (0.5 in). Ten steel spikes were added to the timber layer to ensure that a tension failure mode develops instead of a shear failure, 101.6 mm (4 in) from the end of the beam and 203.2 mm (8 in) between the spikes. The main setup of the composite specimen is shown in Fig. 1.

An MTS computer controlled hydraulic loading system was used to conduct the static load tests. A point load at the midpoint using a 445 kN (100 kip) actuator was applied using stroke control with 2.54 mm $min^{-1}$ (0.1 in/min) loading speed. The loading frame is attached to a strong-floor on which the support fixtures were setup as rollers at each end of the beam. To prevent lateral-torsional buckling, lateral restraining blocks were placed 1.702 m (67 in) from the axis of the vertical supports, with Teflon sheeting added to reduce any friction on the specimen during testing.

For the AE monitoring, seven Brüel & Kjær accelerometer sensors were placed evenly along the beam specimens, as it is shown in Fig. 2. The placements of sensors 2 to 7 are to provide sufficient temporal separation of initial arrival stress waves. The even spatial separation allows triangulation to estimate the location ($x$, $y$ and $z$ coordinates) of the emission in future studies. Sensor 1, positioned in the middle, is used as a trigger to initiate signal recording. The placement of the triggering signal is largely due to the following two reasons:

1. Sensors placed in the middle should have a shorter average time of flight compared to other sensors.
2. The concentrated load is placed in the middle section of the beam, and hence, it is also the region of interest where most emission events are expected to occur.

## 2.2. Acoustic emission signal feasibility analysis

The resultant AE signals are depicted in Fig. 3. From the selected samples, the feasibility analysis of AE emission signal uses the following criteria.

*Fig. 1.* G-C specimen setup

Signal-to-Noise Ratio (SNR): The ambient noise level from each sensor appears to be stationary white noise within the acceptable strength limit. All sensors picked up a certain level of signal. These two results indicate the sensors and the acquisition device are performing nominally.

Sufficient time delay in data recording: All signals are recorded with a specific time delay of 2 ms, even with sensor 1 being the triggering sensor. This setting is validated in Fig. 4. The strong initial amplitude of sensor 4 indicates the emission occurs near the sensor. The emission propagates to sensor 7 with an initial peak of around 0 ms. This result suggests that the AE takes about 1 ms to travel from one end of the beam to the other.

Time Of Flight (TOF) vs. energy response: Energy attenuation is a function of 1/r2. A shorter arrival time is expected to correlate with a stronger signal. From Fig. 4, roughly estimated arrival times of different sensors correlate with the associated energy response. Sensor 5 shows the highest amplitude with the shortest arrival time of all.

This result suggests the emission might have originated from the area near sensor 5. Sensor 4, positioned the furthest from the source, has the longest arrival time and lowest energy response. This result also suggests that the amplitudes of the sensory impulse responses are very similar.

TOF determination: The time of flight determination is crucial to infer the location of the emission. This study employs accelerometers which are wide-band transducers. Hence, the time of flight will be frequency-dependent. Based on the strong SNRs the spectrogram analysis is quite feasible.

Source determination: Based on the result from Figs 3 and 4, all seven sensors perform well, with relevant signal

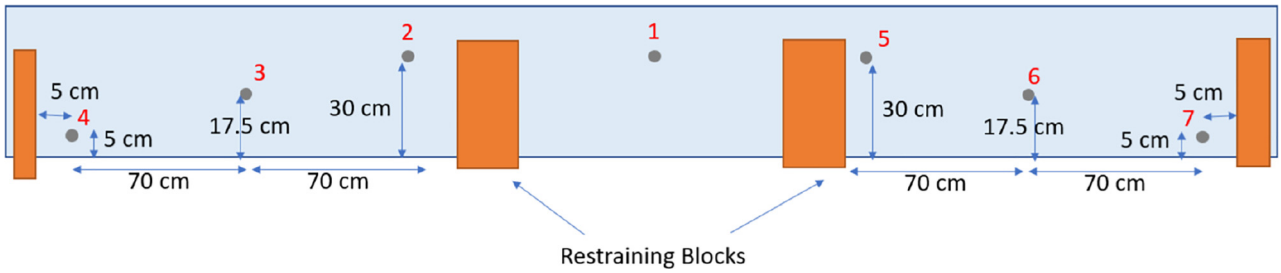


*Fig. 2.* Sensory placement

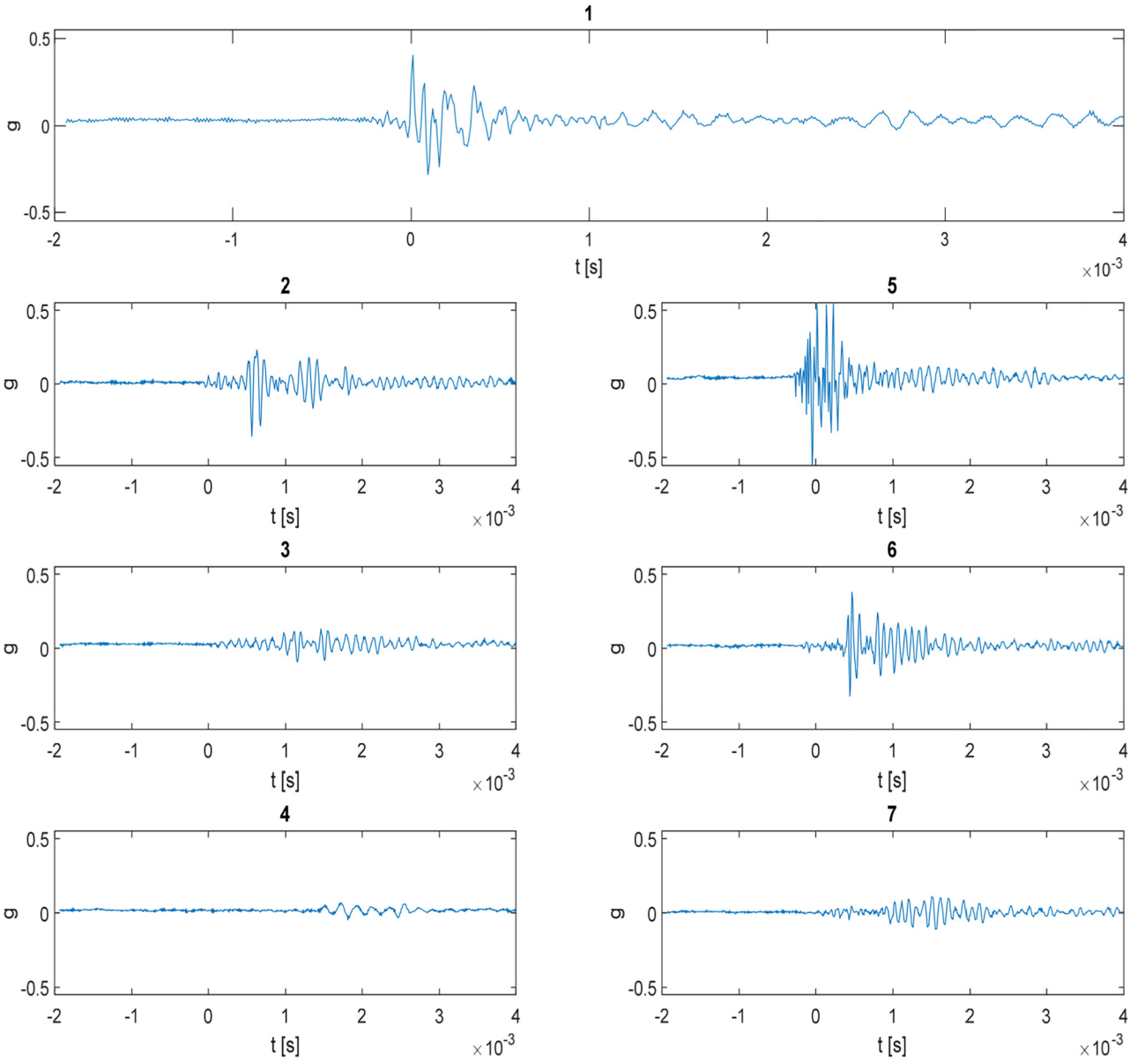


*Fig. 3.* Event 1 signal captured by sensors

processing techniques for obtained TOF. It is possible to determine both $x$ and $z$ directions and the corresponding propagation speed velocities $v_x$ and $v_z$. Simple triangulation should be sufficient to infer AE source location with proper assumptions.

Experiment setup: The bee wax used for the test was not strong enough to hold the sensors in position during the final AE event with much higher amplitude, however a stronger adhesive material would be recommended for future testing. Table 1 shows the results of the signal feasibility analysis.

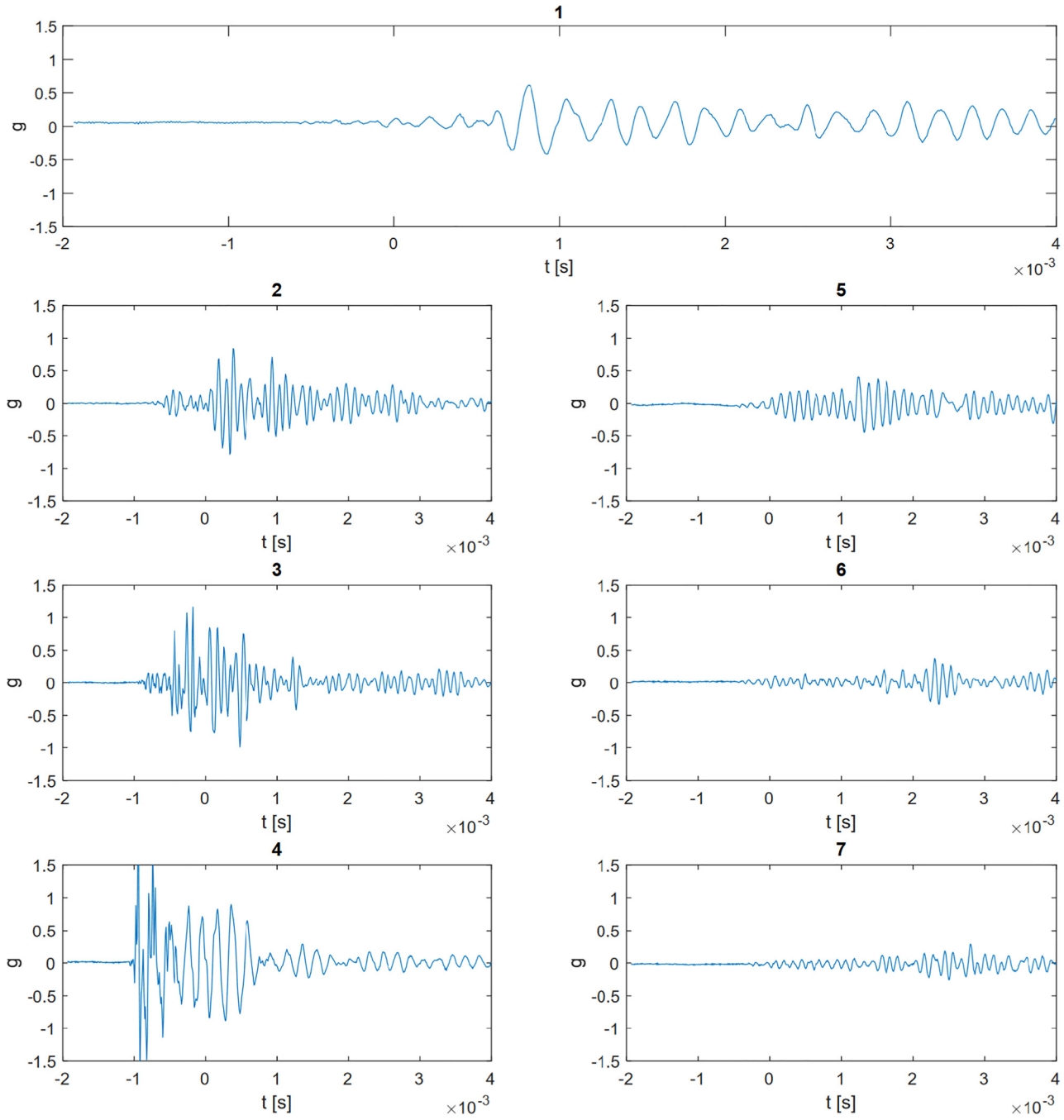


*Fig. 4.* Event 2 signal captured by sensors

*Table 1.* Signal feasibility analysis results

| Signal criteria | Condition |
|---|---|
| Signal-to-Noise | Good |
| Sufficient time delay in data recording: | Good |
| Time of flight (TOF) vs. energy response | Good |
| TOF determination | Good |
| Source determination | Feasible |
| Experiment setup | Good |

## 3. RESULTS

Single-span, simply supported beams may fail either due to bending at midspan or shear at the supports. It is difficult to predict, which failure would occur first, given the inhomogeneity of the composite beam. While increasing the cross-section height of a beam can enhance its bending resistance, it may not necessarily result in a sufficiently larger shear capacity. It is worth noting that bending failure is usually associated with relatively large deflections. On the

other hand, transverse shear can cause splitting and delamination of a timber member near the flexural neutral axis, which can happen suddenly without any warning signs of deformation.

Vertical reinforcing steel bars embedded into concrete beams have been effectively used to prevent shear failure. Likewise in the test, under service loads, the shear rapidly declines and theoretically ceases at midspan, similar reinforcement is required in the vicinity of the supports. The laboratory tests were intended to show that the glued-in spikes would effectively stop the propagation of shear cracks from developing in the glulam, starting from the supports,

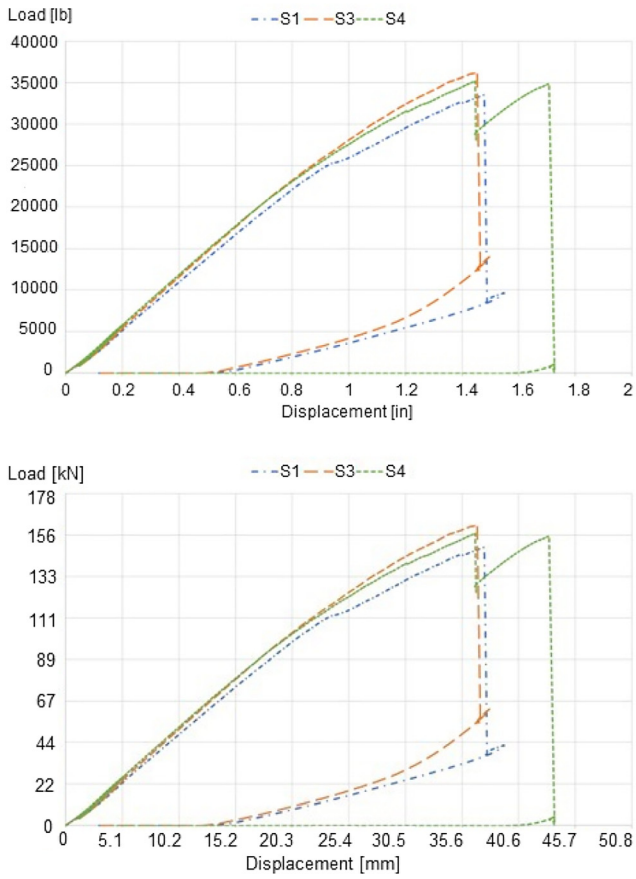


*Fig. 5.* Measured load-displacement diagrams in imperial and converted SI units (1 in = 25.4 mm; 10 lb = 4.448 kN)

*Fig. 7.* Shear failure mode (S3)

Specimen S1 Specimen S4

*Fig. 6.* Tension failure mode

and may result in the splitting of the timber member. Glulam beams can lose strength due to cracks, which can vary in depth, length, and location. These cracks affect the shear strength because they typically run along the grain and glue lines of the beams.

The goal of the test was not to increase the bearing capacity but to be able to control the failure mechanism.

The measured load-displacement diagrams for the three specimens are shown in Fig. 5. Specimens S1 and S4 exhibited tension failure, see Fig. 6, while specimen S3 failed in shear, see Fig. 7.

## 4. CONCLUSIONS

The load test results indicate that the shear spikes presumably contained the shear failure in two of the three beams, allowing for a tension failure mode. The tension failure observed appeared to originate from finger-joints present in the bottom layers of the glulam. The sensitivity of accelerometers provides acceptable level of SNR and the placements of them allow for future analyses in failure model determination and proximity estimation. The AE findings will be presented in an upcoming second paper. Instead of using the standard unbalanced glulam configuration developed for members in bending, a different glulam layering can be adopted, optimized for the mostly tension loading in such G-C composite beams.

## ACKNOWLEDGEMENTS

The research was performed within the framework of the institutional cooperation between the Authors' universities. The authors are grateful to the students who assisted with the laboratory specimen construction and experimental setup.

## REFERENCES

[1] A. Jutila, "Wood concrete composite bridges, Finnish speciality in the Nordic Countries," in *Proceedings of the International Conference Timber Bridges*, Lillehammer, Norway, September 12–15, 2010, pp. 383–392.

[2] J. Negrão, C. D. Oliveira, F. M. M. de Oliveira, and P. Cachim, "Glued composite timber-concrete beams, I: Interlayer connection specimen tests," *ASCE, J. Struct. Eng.*, vol. 136, no. 10, pp. 1236–1245, 2010.

[3] J. H. J. O. Negrao, F. M. M. de Oliveira, C. Oliveira, and P. Cachim, "Glued composite timber-concrete beams, II: Analysis and tests of beam specimens," *ASCE, J. Struct. Eng.*, vol. 136, no. 10, pp. 1245–1254, 2010.

[4] P. L. Clouston and C. P. Quaglia, "Experimental evaluation of epoxy based wood-concrete composite floor systems for mill building renovations," *Int. J. Construct. Environ.*, vol. 3, no. 3, pp. 63–74, 2013.

[5] J. Balogh, "Laminated wood-concrete structural members," *Pollack Period.*, vol. 8, no. 3, pp. 79–86, 2013.

[6] P. Clouston, L. A. Bathon, and A. Schreyer, "Shear and bending performance of a novel wood–concrete composite system," *J. Struct. Eng.*, vol. 131, no. 9, pp. 1404–1412, 2005.

[7] S. Lamothe, L. Sorelli, P. Blanchet, and P. Galimard, "Engineering ductile notch connections for composite floors made of laminated timber and high or ultra-high performance fiber reinforced concrete," *Eng. Struct.*, vol. 211, 2020, Art no. 110415.

[8] R. Steiger, E. Serrano, M. Stepinac, V. Rajčić, C. O'Neill, D. McPolin, and R. Widmann, "Strengthening of timber structures with glued-in rods," *Construct. Build. Mater.*, vol. 97, pp. 90–105, 2015.

[9] Dayton Superior, Sure Bond,™, J58, *Technical Data Sheet*, 2015.

[10] H. R. Hardy, Jr., *Acoustic Emission/Microseismic Activity*. vol. 1, Taylor & Francis, 2003.

[11] I. Szucs, Z. Balogh, and R. Holtzman, "Acoustic emission at failure of steel-timber-concrete composite beams," *Pollack Period.*, vol. 14, no. 2, pp. 193–200, 2019.

[12] V. Nasir, S. Ayanleye, S. Kazemirad, F. Sassani, and S. Adamopoulos, "Acoustic emission monitoring of wood materials and timber structures: A critical review," *Construct. Build. Mater.*, vol. 350, 2022, Art no. 128877.